XI. COGNITIVE INFORMATION PROCESSING*

Academic and Research Staff

Prof. M. Eden
Prof. J. Allen
Prof. F. F. Lee
Prof. S. J. Mason
Prof. W. F. Schreiber
Prof. D. E. Troxel
Prof. T. S. Huang
Dr. R. R. Archer
Dr. W. L. Black
Dr. J. E. Green
Dr. K. R. Ingham
Dr. O. J. Tretiak
F. X. Carroll
C. L. Fontaine
E. R. Jensen
A. J. Laurino
D. M. Ozonoff
E. Peper
Sandra A. Sommers

Graduate Students

G. B. Anderson
T. P. Barnwell III
W. L. Bass
B. A. Blesser
J. E. Bowie
A. E. Filip
A. Gabrielian
A. M. Gilkes
R. E. Greenwood
E. G. Guttmann
R. V. Harris III
D. W. Hartman
A. B. Hayes
L. P. A. Henckels
P. D. Henshaw
M. Hubelbank
W-H. Lee
J. I. Makhoul
G. P. Marston III
G. F. Pfister
D. S. Prerau
G. M. Robbins
S. M. Rose
C. L. Seitz
D. Sheena
W. W. Stallings
R. M. Strong
Y. D. Willems
J. W. Woods
I. T. Young

A. MOIRÉ PATTERNS IN SAMPLING HALFTONE PICTURES

1. Introduction

There has been considerable interest recently in the transmission of newspapers by high-resolution digital facsimile. Newspapers contain two types of materials: texts and halftone pictures. For text materials it has been found[1] that at low resolutions (around 100 points per inch) the digital (binary) picture has a poorer quality than an analog picture of equal resolution, while at high resolutions (greater than 200 points per inch) the two have comparable qualities. For binary transmission, it appears that a resolution of 400 points per inch is adequate for reproducing high-quality text materials.

The sampling rate for halftone pictures is determined by two factors: the number of apparent brightness levels we would like to see and the amount of moiré patterns we can tolerate. To get 64 levels of apparent brightness, we have to sample at a rate 8 times the halftone screen density. For a typical halftone screen density of 85 lines per inch, the corresponding sampling rate will be 680 points per inch. Coincidentally, it has been found experimentally that to avoid the appearance of moiré patterns, it is also necessary to sample at a rate about 8 times the halftone screen density.

*This work was supported principally by the National Institutes of Health (Grants 5 PO1 GM14940-03 and 5 PO1 GM15006-03), and in part by the Joint Services Electronics Programs (U.S. Army, U.S. Navy, and U.S. Air Force) under Contract DA 28-043-AMC-02536(E).

It is of course very desirable to use the same sampling rate for the texts and the halftone pictures. If we are satisfied with a less number of apparent brightness levels (than 64) in the halftone pictures, then we can use 400 samples per point for both the texts and the halftone pictures but for the fact that moiré patterns may appear. It is therefore imperative to study how the moiré patterns are formed and how they may be eliminated. We have previoulsy formulated a frequency-domain theory of moiré formation.[2] The purpose of the present report is to present some experimental results verifying our theory.

2. Frequency-Domain Theory of Moiré Formation

We first review our theory briefly. We model a halftone screen with dot diameter D and density f_h dots per unit length (Fig. XI-1a) by

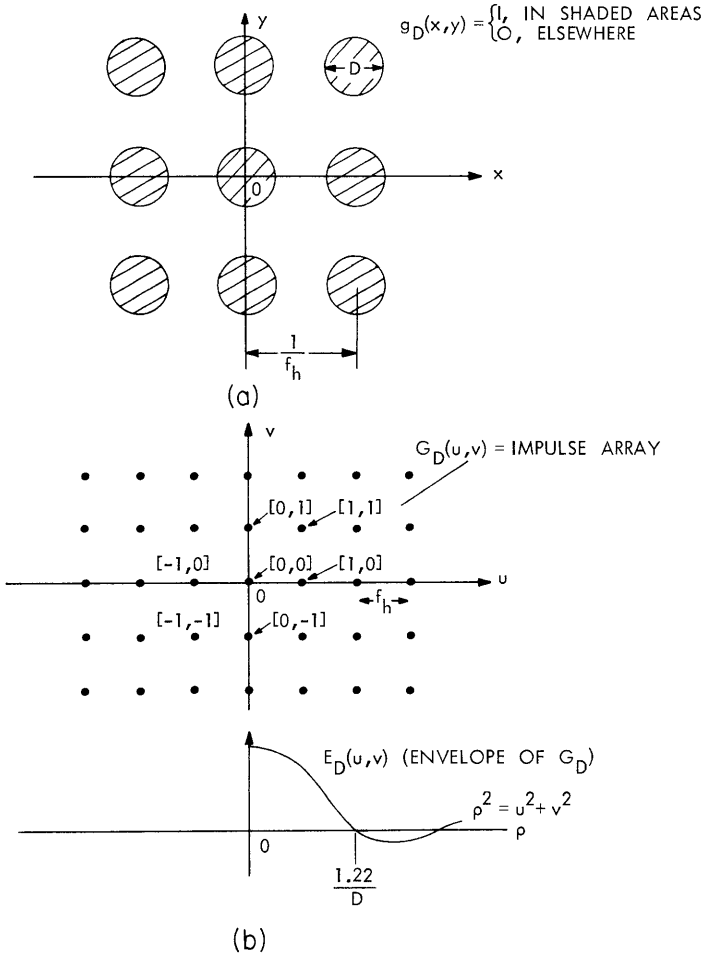

Fig. XI-1. Spectrum of a uniform halftone screen.

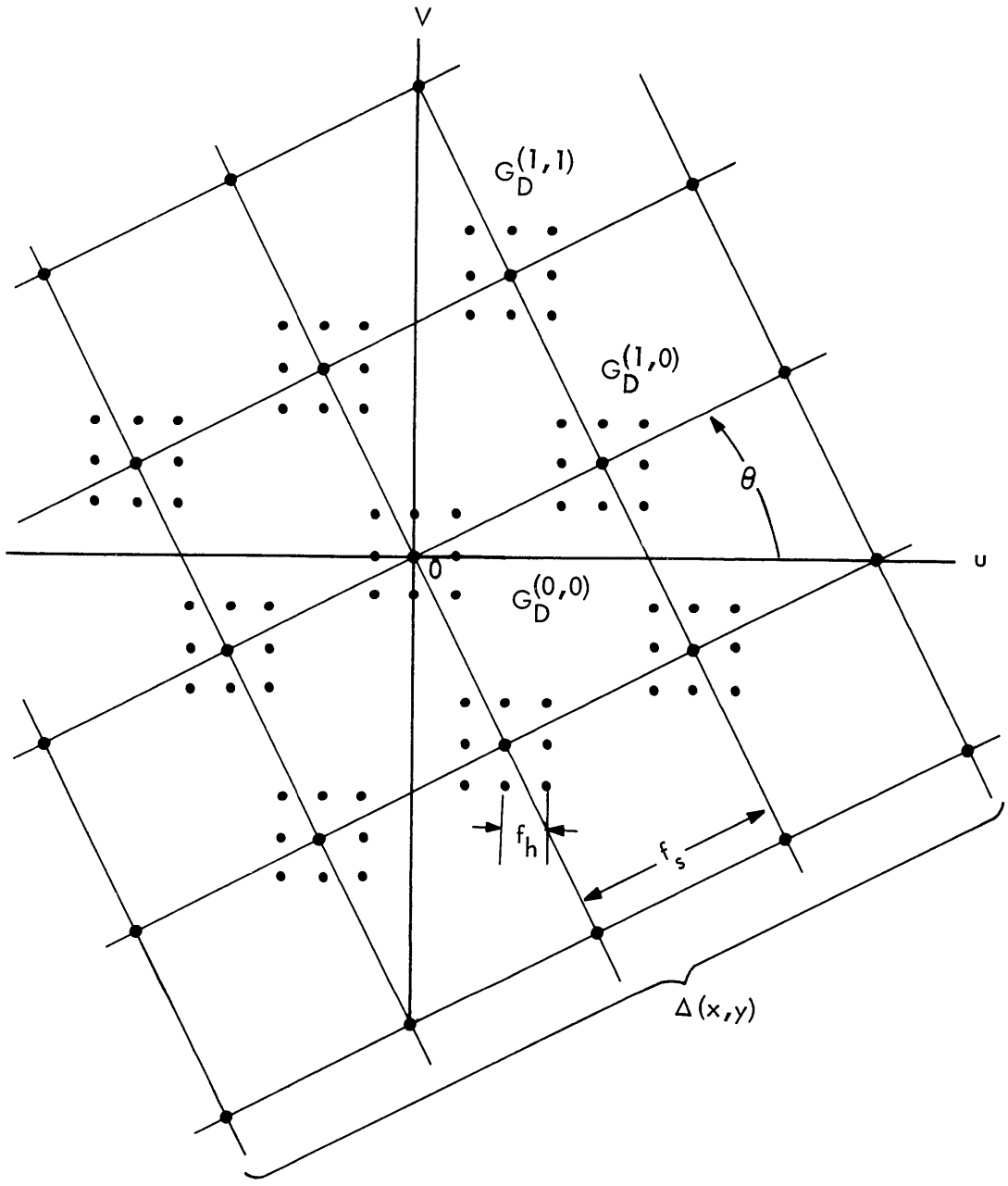

Fig. XI-2. Spectrum of a sampled halftone picture.

(a)

(b)

(d)

(c)

(e)

Fig. XI-3. Sampled halftone pictures.

$$g_D(x, y) = \begin{cases} 1 & \text{if } (x, y) \text{ lies in a dot} \\ 0 & \text{elsewhere} \end{cases} \tag{1}$$

where x and y are spatial coordinates. (We assume that $Df_h \leq 1$.) The Fourier transform, $G_D(u, v)$, of $g_D(x, y)$ is a two-dimensional impulse array (Fig. XI-1b) with period $f_h \times f_h$ and an envelope

$$E_D(u, v) = \frac{\pi D^2}{2} \cdot \frac{J_1\left(\frac{D}{2} 2\pi\rho\right)}{\frac{D}{2} 2\pi\rho} \tag{2}$$

where u and v are spatial frequencies in cycles per unit length, $\rho = \sqrt{u^2 + v^2}$, and $J_1(\cdot)$ is the Bessel function of the first order.

Now we sample the halftone screen with an ideal impulse array $\Delta(x, y)$ which has a period $\frac{1}{f_s} \times \frac{1}{f_s}$. Let θ be the angle between the sampling raster $\Delta(x, y)$ and the halftone screen. Then the Fourier transform of the sampled halftone screen is as shown in Fig. XI-2, where $G_D^{(m, n)}$ are shifted versions of G_D. Any strong components of $G_D^{(m, n)}$ that fall close enough to the origin in the u-v plane will cause moiré patterns. The spatial frequency of the moiré pattern due to a particular component of $G_D^{(m, n)}$ is determined by the vector leading from the origin in the u-v plane to that impulse component.

The discussion above is based on uniform halftone pictures. The result can be applied, however, to nonuniform halftone pictures, since in the latter moiré patterns are most visible in the relatively uniform regions.

3. Some Experimental Results

A halftone picture (f_h = 133 dots per picture width) was scanned at various sampling rates on the new CIPG scanner,[3] with $\theta = 45°$. The resulting sampled pictures are shown in Fig. XI-3. The halftone picture before scanning is shown in Fig. XI-4. The

Fig. XI-4. Halftone picture before sampling.

sampling rates, as well as the moiré frequencies, predicted by our theory are given in Table XI-1. For most part of the halftone picture, we have $Df_h \approx .66$. The relative

Table XI-1. Predicted moiré frequencies.

Picture No.	Sampling Rate (samples per picture width)	Predicted moiré frequencies (cycles per picture width) and responsible components of G_D
Fig. XI-3a	128	60 [1, 1]; 48 [1, 0]
Fig. XI-3b	182	6 [1, 1]; 9 [2, 0]
Fig. XI-3c	246	58 [1, 1]; 51 [3, 0]
Fig. XI-3d	274	86 [1, 1]; 12 [3, 0]
Fig. XI-3e	364	12 [2, 2]; 18 [4, 0]

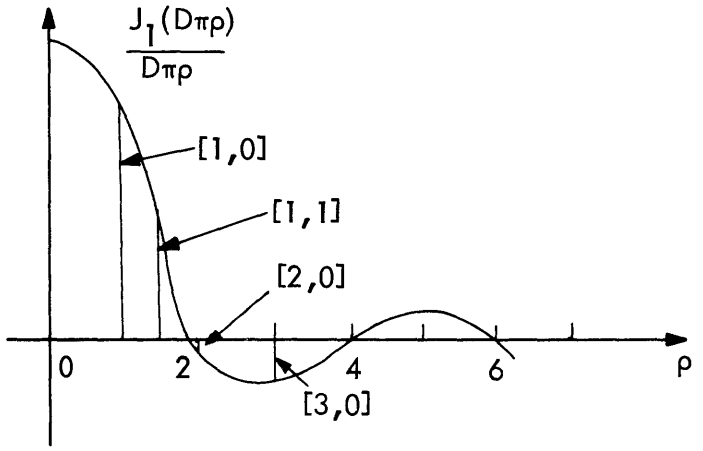

Fig. XI-5. Relative strength of components of G_D for $Df_h = .66$.

strength of the components (m, n) of G_D (cf. Fig. XI-1b) for this particular case can be seen from the sketch in Fig. XI-5. It will be seen that the appearance of the moiré patterns in Fig. XI-3 conforms to the predictions in Table XI-1 and Fig. XI-5.

T. S. Huang, G. B. Anderson, J. W. Woods

References

1. W. F. Schreiber, "Reproduction of Graphical Data by Facsimile," Quarterly Progress Report No. 84, Research Laboratory of Electronics, M. I. T., January 15, 1967.
2. T. S. Huang, "Digital Transmission of Halftone Pictures," E G & G Technical Report No. B-3945, January 31, 1969.
3. W. F. Schreiber, The New Scanner, unpublished memorandum, Research Laboratory of Electronics, M. I. T., 1968.

B. HOLOGRAPHY AND IMAGING OF THREE-DIMENSIONAL OBJECTS

The Fresnel approximation for the scalar wave equation enables the reduction of many diffraction problems to manageable form.[1] It is applied to obtain a simple model for the propagation of coherent light through an optical system. We shall apply an extension of this sort of analysis to model some problems in which images of three-dimensional objects are obtained.

1. Problem Formulation and Light-Matter Interaction

Suppose that we have an object illuminated by a coherent wave front emanating from point P_o (Fig. XI-6). We would like to know the value of the field at point P_1. The field is monochromatic and is modeled by the scalar wave equation

$$\nabla^2 f + \left(\frac{2\pi}{\lambda}\right)^2 f = \mathcal{J}. \tag{1}$$

In Eq. 1, f is the field variable, and $\mathcal{J}$ is the source distribution. We model the interaction between the field and the object by supposing that there is a source distribution coupled to the field given by

$$\mathcal{J}_d(x, y, z) = a(x, y, z)\, f(x, y, z). \tag{2}$$

In this equation, $\mathcal{J}_d$ is the induced source distribution, and a(x, y, z) is the property of the object, such as conductivity or polarizability, that couples to the field. This model, except for ignoring effects that are peculiar to a vector wave equation, is not an unreasonable one for the analysis of light propagation. Unfortunately, it leads to

$$\left\{\nabla^2 + \left(\frac{2\pi}{\lambda}\right)^2 - a(x, y, z)\right\} f = \mathcal{J}_i(x, y, z). \tag{3}$$

We have lumped the action of the object into the differential operator, so that the term on the right side of the equality sign is just the independent source. There seem to be no general techniques for handling this sort of equation. The following procedure may be tried.

Let f_o be the solution to

$$\left(\nabla^2 + \left(\frac{2\pi}{\lambda}\right)^2\right) f_o = \mathcal{J}_i \tag{4}$$

with no material present. A new distribution is found by multiplying the constituent function by f_o, and a second field distribution is found for this. This sequence may be

$$\mathcal{J}_1 = f_o \cdot a$$

$$\left(\nabla^2 + \left(\frac{2\pi}{\lambda}\right)^2\right) f_1 = \mathcal{J}_1 \tag{5}$$

repeated, with the iteration step being given by (6). This equation also contains the solution hoped for

$$S_k = f_{k-1} \cdot a$$

$$\left(\nabla^2 + \left(\frac{2\pi}{\lambda}\right)^2\right) f_k = S_k \tag{6}$$

$$f = \sum_{k=0}^{\infty} f_k.$$

If a is small in the sense

$$|a| \ll 1$$

$$\int a(x, y, z)\, dxdydz \ll 1, \tag{7}$$

we may hope to approximate f by

$$f = f_o + f_1. \tag{8}$$

We shall use this approximation from now on.

2. Fresnel Approximation

Suppose that the object is illuminated by a point source located at P_o. We shall represent three-space coordinates by the vector $\vec{r}$. The field that is due to the source is given by

$$f_o = \frac{A\, e^{i\frac{2\pi}{\lambda}|\vec{r}-\vec{r}_o|}}{|\vec{r}-\vec{r}_o|}, \tag{9}$$

with A the intensity of the source, and r_o the coordinates of the source. By applying the reciprocity theorem for radiation, we find that the field at point P_1 caused by the induced sources is given by

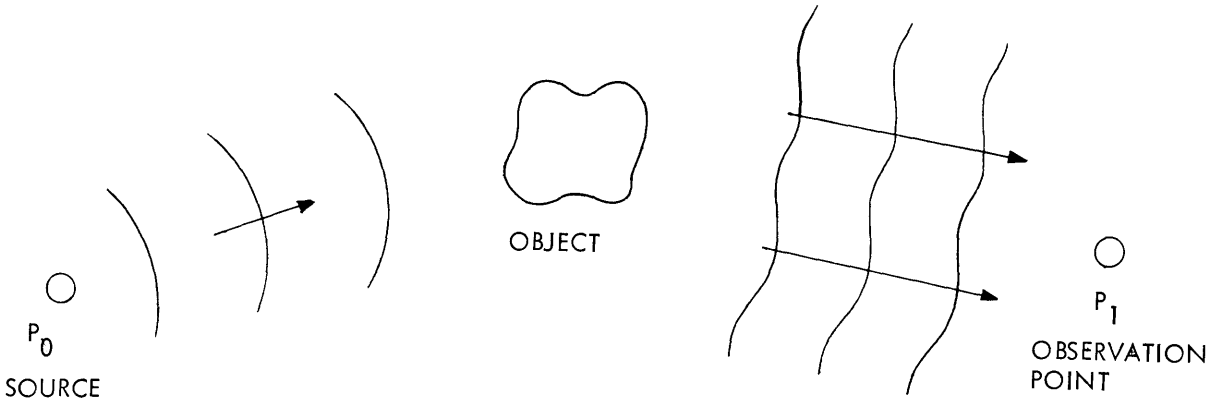

Fig. XI-6. Diffraction by an object.

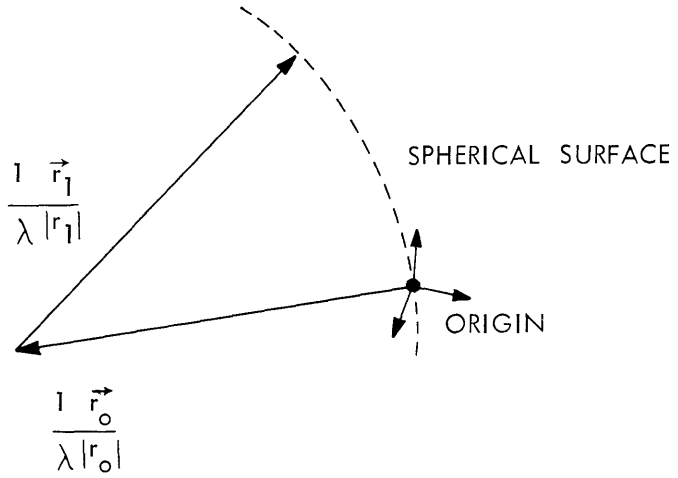

Fig. XI-7. Transform coordinates.

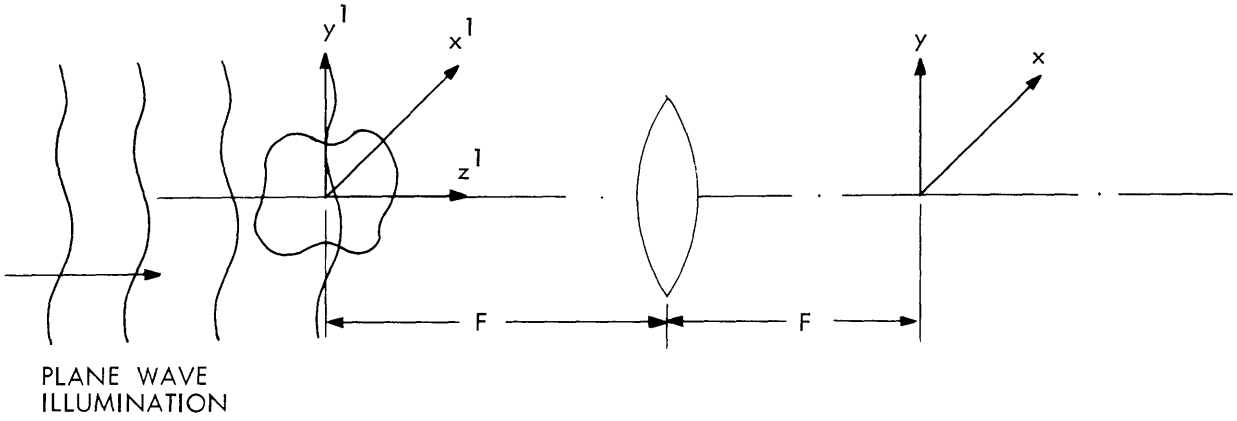

Fig. XI-8. Fourier transform system.

$$f_1(\vec{r}_1) = A \int d\vec{r}\; a(\vec{r})\, \frac{e^{i\frac{2\pi}{\lambda}|\vec{r}-r_o|}\; e^{i\frac{2\pi}{\lambda}|\vec{r}-r_1|}}{|\vec{r}-r_o||\vec{r}-r_1|}. \tag{10}$$

We may simplify this by expanding the exponential function in a power series in $\vec{r}$. If the range over this expansion is valid it is small enough so that the $|\vec{r}-r_o| \cdot |\vec{r}-r_1|$ does not change much, and if

$$\left(\frac{2\pi}{\lambda}\right)^2 \gg \frac{1}{|\vec{r}_1|} \cdot \frac{1}{|\vec{r}_o|},$$

the expansion takes the form given in (11).

$$f_1(r) = \left(\int a(r)\, g(r)\, dr\right) \frac{A\, e^{i\frac{2\pi}{\lambda}(|r_o|+|r_1|)}}{|r_o||r_1|}$$

$$g(r) \cong \exp\left(\frac{2\pi i}{\lambda}\left(-\vec{u}\cdot\vec{r} + \frac{1}{2}\left(\left(\frac{1}{r_o}+\frac{1}{r_1}\right)\vec{r}^2 - \frac{(\vec{r}_o\cdot\vec{r})^2}{|r_o|^3} - \frac{(\vec{r}_1\cdot\vec{r})^2}{|r_1|^3}\right)\right)\right)$$

$$\vec{u} = \left(\frac{\vec{r}_o}{r_o}+\frac{\vec{r}_1}{r_1}\right). \tag{11}$$

This may be interpreted as follows.

The wave that is due to the object is found by multiplying the object function by a quadratic phase factor having the form

$$\exp\left(\frac{\pi i}{\lambda}\left(\left(\frac{1}{|r_o|}+\frac{1}{|r_1|}\right)\vec{r}^2 - \frac{(\vec{r}_o\cdot\vec{r}_1)^2}{|r_o|^3} + \frac{(\vec{r}_1\cdot\vec{r})}{|r_1|^3}\right)\right) \tag{12}$$

and taking the three-dimensional Fourier transform of this product for the transform variable given by

$$-\left(\frac{\vec{u}}{\lambda}\right). \tag{13}$$

3. Special Cases

Special cases arise when Eq. 11 reduces to a normal Fourier transform. This is true if $\vec{r}_o$ and $\vec{r}_1$ approach infinity. Under these conditions, it is relevant to note that

the transform parameter $\vec{u}$ is composed of the observation and illumination direction vectors. If the illumination vector is fixed and the observation point is varied, the values for which the Fourier transform is found are shown in Fig. XI-7. This analysis applies to x-ray diffraction.

The same conditions are met if the light disturbed by the object is observed in the back focal plane of a lens, as shown in Fig. XI-8. If the coordinate system of the object coincides with the front focal point on the axis of symmetry, the function f_1 on the back focal plane is given in

$$f_1(x, y) = \hat{a}\left(-\frac{x}{\lambda F}, -\frac{y}{\lambda F}, \frac{(x^2+y^2)}{2\lambda F^2}\right). \tag{14}$$

The function $\hat{a}$ is the three-dimensional transform of $a(x', y', z')$. If we may treat the third argument as zero, then $f_1(x, y)$ is the two-dimension transform of the function obtained by integrating $g(x', y', z')$ along z'.

The principal value of this formulation is that it suggests approaches for analyzing the relationship between the wavefront recorded in a system and the three-dimensional object that caused it.

O. J. Tretiak

References

1. J. W. Goodman, Introduction to Fourier Optics (McGraw-Hill Book Company, New York, 1968), pp. 77-112.

C. SURVEY OF TYPE FONT USAGE

1. Introduction

One of the major projects now under way in our group involves the construction and testing of a reading machine for the blind. The machine on which work is being done at the present time includes a page reader and is capable of being trained to recognize a large number of type fonts. Because normalizing operations are carried out in the character-recognition algorithms that are employed, the machine is not bothered by variations in print size for a given typeface as long as the height-to-width ratio remains unchanged; for example, once it has been trained to recognize 10-point CENTURY it will also be able to recognize 14-point CENTURY.

Initial training and debugging of software and hardware have been done with 14-point TEXTYPE. The reading machine is now ready to be trained on other type fonts. To learn which type fonts should be employed in the training, the following survey of American publishers was carried out.

Table XI-2. Current usage of type fonts.

TYPE FONTS	PERCENTAGE OF TOTAL PRODUCTION (1968) ACCOUNTED FOR
TIMES ROMAN CALEDONIA BASKERVILLE	62%
CENTURY JANSON ELECTRA FAIRFIELD	26%
GRANJON IMPRINT BODONI PRIMER MODERN HELVETICA OPTIMA GOTHIC SPARTAN (FUTURA)	9%
BOOKMAN GARAMOND OLD STYLE CASLON MONTICELLO BEMBO PALATINO SCOTCH PERPETUA MELIOR TEXTYPE UNIVERSE BULMER DEVINNE	3%
TOTAL	100%

2. The Survey

Sixty of the major publishing houses in the United States were sent questionnaires in which they were asked to list the ten type fonts that they used most during the past year in printing hard-cover books, and to indicate the approximate percentage of their production accounted for by each of the fonts, and the number of books (the total number of copies) printed during the year for which the statistics were given. Replies were received from 40 publishers, whose annual production ranged from 30,000,000 to 2500 copies. The total production reported was approximately 130,000,000 copies, but only 80,000,000 was used in arriving at the statistics given in Table XI-2 in this report, since some of the replies were incomplete.

Since most publishers do not keep detailed records on type-font usage, the statistics in Table XI-2 are very approximate. Typefaces are listed in order with respect to apparent popularity, and broken arbitrarily into four major groupings with respect to current usage. It is encouraging to note that only 30 type fonts were mentioned in the replies, and of those, 3 alone account for some 62% of last year's production.

Many publishers took the time and trouble to enclose helpful comments with their replies. Some of these comments were the following.

1. It is common practice to use different typefaces for chapter display material, subheadings, and tabular material, and to mix sans serif with serif faces. Universe, Helvetica, Melior, Optima, Gothic, and Old Style are commonly used as display faces.

2. The popularity of typefaces changes from year to year and varies from one country to another. In Europe, Bembo has been very popular for many years, while in the United States it is low down on the list. Some other typefaces currently in vogue in Europe are: Times Roman, Baskerville, Imprint, Garamond, Ehrhardt, Plantin, and Bell.

3. There are definite differences between typefaces with the same name in different composing systems. For example, Linotype Garamond is different from Intertype Garamond.

4. The most popular type font for paperbacks (not covered in our survey) appears to be Times Roman.

3. Conclusion

While the statistics obtained from our survey are approximate, they do tell us what we need to know in order to begin training the reading machine to recognize more type fonts. Clearly, Times Roman, Caledonia, and Baskerville should be among the first group of fonts used in the training program.

G. P. Marston III, L. P. A. Henckels